



Parameters Optimisation in the Vibration-based Machine Learning Model for Accurate and Reliable Faults Diagnosis in Rotating Machines

DOI:
[10.3390/machines8040066](https://doi.org/10.3390/machines8040066)

Document Version
Final published version

[Link to publication record in Manchester Research Explorer](#)

Citation for published version (APA):

Espinoza Sepulveda, N., & Sinha, J. (2020). Parameters Optimisation in the Vibration-based Machine Learning Model for Accurate and Reliable Faults Diagnosis in Rotating Machines. *Machines*.
<https://doi.org/10.3390/machines8040066>

Published in:
Machines

Citing this paper

Please note that where the full-text provided on Manchester Research Explorer is the Author Accepted Manuscript or Proof version this may differ from the final Published version. If citing, it is advised that you check and use the publisher's definitive version.

General rights

Copyright and moral rights for the publications made accessible in the Research Explorer are retained by the authors and/or other copyright owners and it is a condition of accessing publications that users recognise and abide by the legal requirements associated with these rights.

Takedown policy

If you believe that this document breaches copyright please refer to the University of Manchester's Takedown Procedures [<http://man.ac.uk/04Y6Bo>] or contact uml.scholarlycommunications@manchester.ac.uk providing relevant details, so we can investigate your claim.



Article

Parameter Optimisation in the Vibration-Based Machine Learning Model for Accurate and Reliable Faults Diagnosis in Rotating Machines

Natalia Espinoza Sepulveda ¹ and Jyoti Sinha ^{1,*}

¹ Dynamics Laboratory, Department of MACE, The University of Manchester, Manchester M13 9PL, UK; Natalia.Espinozasepulveda@manchester.ac.uk

* Correspondence: Jyoti.Sinha@manchester.ac.uk

Received: 24 September 2020; Accepted: 22 October 2020; Published: 23 October 2020

Abstract: Artificial intelligence (AI)-based machine learning (ML) models seem to be the future for most of the applications. Recent research effort has also been made on the application of these AI and ML methods in the vibration-based faults diagnosis (VFD) in rotating machines. Several research studies have been published over the last decade on this topic. However, most of the studies are data driven, and the vibration-based ML (VML) model is generally developed on a typical machine. The developed VML model may not predict faults accurately if applied on other identical machines or a machine with different operation conditions or both. Therefore, the current research is on the development of a VML model by optimising the vibration parameters based on the dynamics of the machine. The developed model is then blindly tested at different machine operation conditions to show the robustness and reliability of the proposed VML model.

Keywords: vibration-based faults diagnosis (VFD); artificial intelligence (AI); machine learning (ML); artificial neural network (ANN); vibration-based condition monitoring (VCM)

1. Introduction

Rotating machines of different types are commonly used in industries. Therefore, their availability and reliability are important considerations to avoid any unplanned down time for plants. There are many rotating machines, for example, turbogenerator sets in the power plants, that are critical assets. Any failure of these assets may have an impact on plant safety in addition to production losses due to unplanned shutdown. Condition monitoring, typically vibration-based condition monitoring (VCM) [1,2], is a well-accepted and adopted practice to monitor critical machines and assets to identify the defects/faults at early stages of occurrence to avoid failures and unnecessary production losses, and also to maintain the plant safety. Although the VCM is a well developed technique [1,2] the fault detection process is generally complex and requires significant experience and engineering judgement. Often, there are many identical machines used within a plant to meet their requirements. This makes the fault detection process even more complex from one machine to another identical machine. This is due to either their different dynamics or different operation speeds or both. Different dynamics are generally observed mainly due to little difference in their installation structures (foundations) [3,4].

Artificial intelligence (AI)-based machine learning (ML) models seem to be the future for most applications [5]. Recent research effort has also been made regarding the application of these AI and ML methods in the vibration-based faults diagnosis (VFD) in the rotating machines [6]. Several research studies have been published over the decade on this topic, covering a wide range of techniques implemented by processing different vibration parameters. Moreover, most of the studies

are data driven, and the vibration-based ML (VML) model is generally developed on a typical machine, under specific operational conditions.

Some studies [3,4] have been conducted on the development of the ML model for rotor-related faults diagnosis using principal component analysis (PCA). This method combines data from identical machines with different foundations and operating at different speeds together in their ML models. The PCA method is used mainly to reduce the dimension of the analysed parameters to simplify the diagnosis processes. Moreover, these models are not tested when the machine is operating at different operating conditions and/or installed on a different foundation other than that are used in the training of the ML models.

There are also many studies on the development of ML models [7–13] for anti-friction bearing defects diagnosis only. Some studies [7,8] have used the PCA method for the bearing faults diagnosis. De Moura et al. [9] have used both the PCA and artificial neural network (ANN) methods to develop their ML models. They have demonstrated that the ML model based on the ANN performs better than the PCA-based ML model. The studies by Shen et al. [10] and Chen et al. [11] have used all possible defects (roller, inner race and outer race defects) to develop their ML models for the bearing fault diagnosis. Shen et al. [10] have used the support vector regression machines (SVRMs) method, whereas the convolutional neural network (CNN) method was used by Chen et al. [11]. Zhang et al. [12] have used different bearing faults and different operational conditions together to develop the ML model using ANN approach. A supervised decision tree is proposed by Song et al. [13] for the bearing defect diagnosis at different machine speeds.

Similarly, the ML models are available in the literature to identify both bearing and gearbox defects [14–16] and the defects in gearboxes only [17,18]. These studies have used different methods such as a twin support vector machine (TWSVM) [14], the deep learning neural network method [15], a CNN [16], PCA [17] and a support vector machine (SVM) [18]. The application of smart fault detection models is also extended to different fault detections in the compressors [19] and pumps [20,21] other than bearing and rotor defects.

Walker et al. [22] have used an ANN to perform rotor unbalance estimation. Mohamed et al. [23] have studied the detection of shaft cracks with different depths from 0% to 60% in shaft diameter. Nahvi and Esfahanian [24] have used ANN-based VML models for multiple rotor-related faults detection. However, validation conducted with a few cases has shown variable results depending on the fault position [24].

A summary of the above studies published over the past decade is also listed in Table 1. These studies have used different vibration parameters in the development of VML models. It is also important to note that most of the studies have only used a few types of faults in the rotating machines. These VML models in the literature are generally developed using the training data from a particular machine with known faults and operation conditions. Therefore, the diagnosis by these models may work well on the machine with same operating conditions for the faults used in the training. However, it is difficult to know whether each of these models can work well for all types of machine faults. These developed VML models are also not tested to predict the faults accurately if applied blindly on the other identical machines or a machine with different operation conditions or both. Therefore, it is difficult to rely on such an VML model without involving experience and engineering judgement in faults diagnosis.

The current research is to develop a VML model by optimising the vibration parameters based on the dynamics of the machine. This means that the parameters based on the physics of machine dynamics should be selected. Therefore, the selected parameters are likely to be better indicators for each machine fault to ensure the development of a reliable and robust VML model. In the current study, the parameters, both in time and frequency domains, are kept simple, such as Root Mean Square (RMS), Kurtosis, 1x (one time speed) and its higher harmonics and sub-harmonics [1,2]. These parameters are developed based on the physics of machine dynamics. These parameters have been used in the industry for decades for fault diagnosis [1,2]. Therefore, complex signal processing techniques are not used in the current study. However, the parameters are judiciously selected, thus, developed VML model can also be useful for different faults and other machines. The developed

VML model at a machine speed is then blindly tested at the different machine operation conditions to show the robustness and reliability of the proposed model.

Table 1. A summary of few machine learning (ML) studies for the vibration-based faults diagnosis (VFD) in rotating machines.

Ref. No.	Defects/Faults	ML Method
[3,4]	Several rotor-related defects separately tested at a few different machine speeds and different machine foundations	Principal Component Analysis (PCA) method used to develop the diagnostic model for each speed, each foundation and their combination
[7]	Roller bearing outer race defect only	Probabilistic principal component analysis (PCA)
[8]	Different bearing faults (outer, inner race, rolling element) separately and combined tested at three different machine speeds	PCA and broad learning methods are used for diagnosis. Separate model is used for each speed
[9]	Outer race bearing defect at three different severities, tested at two machine speeds	PCA and ANN methods are used separately. Separate model developed for each speed. ANN performance found to be much better compared to PCA
[10]	Different bearing faults (outer, inner race, rolling element) separately	Support vector regression machines (SVRMs)
[11]	Rolling bearings fault (inner race, outer race, ball, and some combinations)	Convolutional neural network
[12]	Several bearing-related faults at different operational conditions (fault size, motor load, rotor speed)	Transfer learning in ANN
[13]	Roller bearing defects (outer, inner race, rolling element) in low-speed rotating machinery. Different operational speeds, separately	Supervised decision tree
[14]	Bearing faults and bevel gear, separately	Twin support vector machine (TWSVM)
[15]	Planetary gearbox and motor bearings faults, separately	Deep learning neural network
[16]	Bearing faults and gearbox faults, separately	Convolutional neural network
[17]	Gear crack with different severities	PCA and sequential probability ratio test
[18]	Gearbox healthy and three faults types tested at four machine speeds	Support Vectors Machine (SVM) method used, but all speed data are used together for the development of the model
[19]	High and low imbalance in high-pressure cylinder of synthetic ammonia compressor	k-nearest neighbour (kNN)
[20]	Impeller cracks and blockage in pumps	SVM
[21]	Blockages and cavitation in centrifugal pumps	SVM
[22]	Unbalance localisation, two-plane balancing at two different speed	ANN method used separately for each speed
[23]	Rotor crack	ANN
[24]	Several defects through different machines	ANN method used separately for different machines

The recent research studies by Espinoza Sepulveda and Sinha [25] and Luwei, Sinha et al. [26] are used as the basis for further development. The ANN approach is used as the AI-based ML tool for this study. The method is developed on an experimental rotating rig. Espinoza Sepulveda and Sinha [25] have used only time domain parameters in the VML model, which work well for the same machine conditions. Similarly, the time and frequency domain parameters suggested by Luwei, Sinha et al. [26] are also used to develop the AI-based VML model. Once again, this model performed

accurately when tested at the same machine conditions that are used during training. However, both models fail to give an accurate diagnosis when applied to the same machine but at a different speeds. Therefore, the current study further optimised the parameter selection based on the physics-based machine dynamics to develop the VML model using healthy and different faulty conditions of the machine at a different rotating speed. Then, this VML model is used for the fault diagnosis when the machine is operating at a different speed. This test is carried out blindly without further adjustment and training to the developed VML model to show the usefulness of the appropriate optimised parameters used in the development of the reliable AI-based VML model.

The paper presents the parameter selection and optimisation, the VML development for the faults diagnosis at a machine speed, and the results and observations on the blind application of the VML model at a different speed.

2. Machine Learning (ML) Model Development

The artificial neural network (ANN) approach is used to develop a VML model for fault diagnosis in rotating machines. ANNs are systems based on knowledge, which is generated by a training process that creates a correlation, in this case, between symptoms and their correspondent causes [27]. In this study, a multi-layered perceptron (MLP) network structure (Figure 1) is proposed by introducing a hidden layer of weights between the inputs and the outputs [28]. The MLP is used to perform pattern recognition and classification from the vibration data as inputs.

The network parameters, such as a number of layers, a number of neurons and types of functions used at the different stages, are adjusted by iterations and defined in order to obtain an accurate performance. This results in a feedforward network with four hidden layers, each of them with a variable quantity of nonlinear neurons, namely 1000, 100, 100 and 10, from layer 1 to 4, respectively. These details are also shown in Figure 1. The selected functions that are used are as follows: the transfer function at the hidden neurons is the hyperbolic tangent sigmoid [29]; the transfer function at the output neurons is softmax [30]; the training function is scaled conjugate gradient backpropagation; and the performance function is cross-entropy from Matlab. The input layer moves forward along the hidden layers, finishing with the result delivery from the decision layer, which has five possible classes as outputs relating to five rig conditions, namely, healthy, misalignment, shaft bow, looseness and rub.

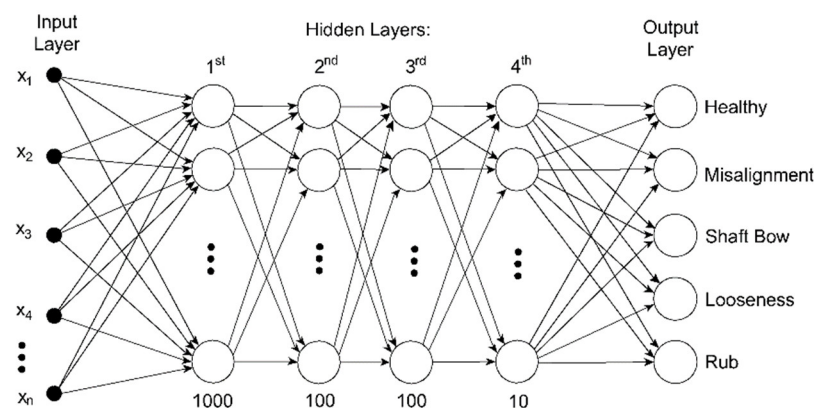


Figure 1. A typical multi-layer perceptron (MLP) neural network used in the study.

The samples (runs) listed in Table 2 are divided into three data sets for the ML model training, validation and then testing [28]. A set of 70% of the samples (runs) from each machine condition (Table 2) at 1800 RPM are used for training the network and modifying the weights according to the learning rule. A total of 15% of the samples is further used for validation, which is conducted by verifying the trained network with these samples until their classification error reaches a desired point of minimum error, giving the order to stop the training process. At this point, the weights are

optimal for the network, and the last group of unknown remaining data (15%) is then tested, providing the generalisation of the network.

Table 2. Data samples per rotor condition and operational speed.

Rotor Condition	No. of Data Sets (Runs) per Rotor Speed	
	1800 RPM (30 Hz)	2400 RPM (40 Hz)
Healthy (residual unbalance)	66	44
Misalignment	109	119
Shaft bow	202	183
Looseness in pedestal	190	87
Rotor rub	112	114

The model performance is calculated as in Equation (1). The error means that the model diagnosis is not accurate on a few occasions. If the healthy condition is diagnosed as faulty, then it may be acceptable. This can be further examined to confirm the model diagnosis. This false diagnosis may not have an impact on plant safety. However, the diagnosis of the faulty conditions as healthy is not acceptable at any cost. Therefore, the VML model must be accurate at least for the healthy condition.

$$\%Performance(or \%Diagnosis) = \frac{No.correct\ classifications}{total\ inputs} 100\% \quad (1)$$

3. Experimental Rig

The measured vibration data from an experimental rotating rig are used in the study [4]. A schematic of the rig is shown in Figure 2. It consists of two steel shafts (Sh1 and Sh2) with a 20 mm diameter coupled through a rigid coupling (C2) and supported through four grease-lubricated 20 mm internal diameter SKF (FY 20TF) flanged ball bearings (B1 to B4) on the flexible bearing pedestals (P1 to P4). The shaft (Sh1) that is 1.0 m in length is connected to a three-phase electric motor (0.75 kW, 3000 RPM maximum) by a flexible coupling (C1). The shaft is carrying two balancing discs (D1 and D2), while the second shaft (Sh2) with a length of 0.5 m is carrying a balancing disc (D3). The balance disc dimensions are 125 mm in diameter and 14 mm in thickness. The flexible bearing pedestals (P1, P2, P3, and P4) are secured by bolts to a steel base that acts as rigid base foundation of the machinery with a high mass. The measured natural frequencies [4] of the rig are 50.66 Hz, 56.76 Hz, 59.2 Hz and 127 Hz, and their mode shapes are shown in Figure 3. The measurement locations for the modal tests used by Nembhard, Sinha et al. [4] are also marked as a1 to a9 in Figure 2 of the rig.

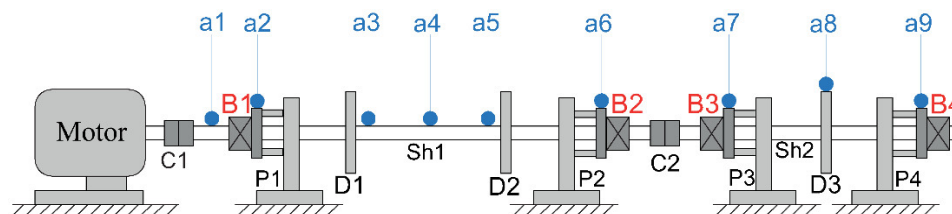


Figure 2. Schematic of the experimental rig.

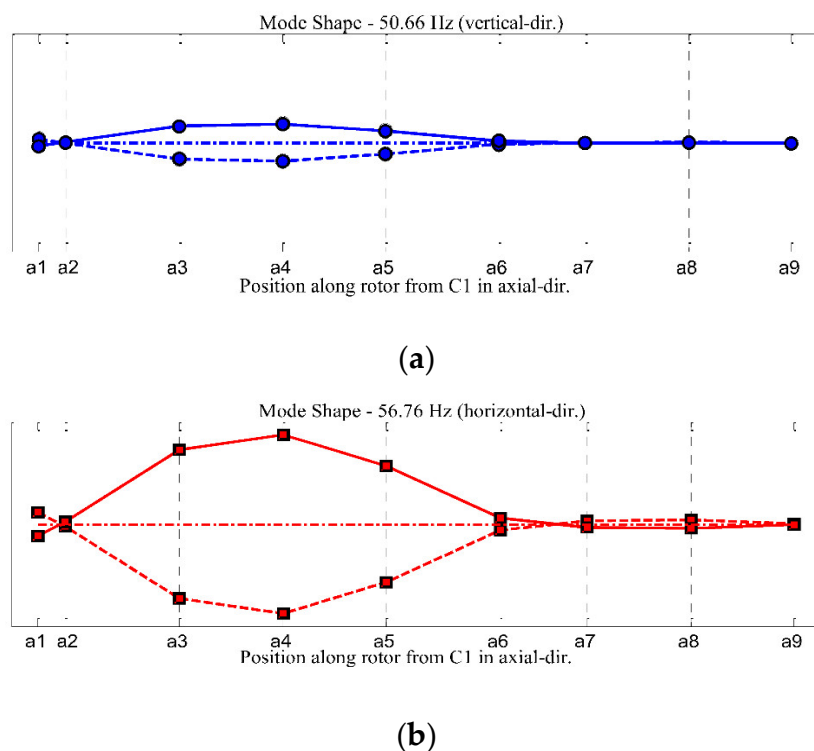


Figure 3. Experimental mode shapes: (a) 50.66 Hz, vertical direction dominant; (b) 56.76 Hz, horizontal direction dominant.

4. Experimental Data and Their Analyses

The measured vibration acceleration data at the bearing housings are available at the rotor speeds of 1800 RPM (30 Hz) and 2400 RPM (40 Hz) for the rotor conditions from healthy (with residual unbalance and possibly little misalignment) to the different faulty conditions [4]. The data details are listed in Table 2. The accelerometers of sensitivity at 100 mV/g and a frequency range of up to 10 kHz are used. The accelerometers are mounted at each bearing housing at an angle of 45 degrees from both vertical and horizontal directions for these experiments [4]. This is shown in Figure 4. The measured vibration data are collected to the PC through a 16-bit data acquisition device at a sampling frequency of 10 ksamples/s [4].

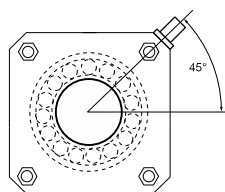


Figure 4. A typical mounting arrangement of an accelerometer at a bearing housing.

Initially, the measured vibration data are analysed in both time (RMS and Kurtosis) and frequency (spectrum) domains. These analyses are commonly used techniques in the industries [1,2]. The spectrum analysis is carried out in the vibration velocity, which is useful for rotor faults detection [1,2].

4.1. Machine Speed: 1800 RPM

Figure 5 shows the time domain (RMS and Kurtosis) and frequency domain features (1x amplitude) for all 66 sets (66 runs) for the healthy condition. The values are nearly stable and constant at each bearings for all sets, as expected. Only 1x values are shown because the health spectra are dominant at 1x only. Figures 6–9 show similar trends for the faulty conditions from misalignment, looseness, shaft bow and shaft rub, respectively. These figures also include the trend of velocity at 2x

and 3x amplitudes along with 1x amplitude. This is because the faults generally generate higher harmonics and subharmonics depending upon fault types [1,2]. The misalignment condition represents the misalignment between the motor shaft and the long shaft (Sh1) near the bearing B1. However, the faulty (looseness, bow and rub) conditions at a speed of 1800 RPM consist of two cases which are clearly seen in Figures 7–9. Looseness represents looseness in the bearing pedestal P3 at 2 different levels; similarly, rub near disc D1 with two different clearances between the rotor and stator, and the shaft bow in the long shaft and short shaft are separately simulated in the experiments. It is also obvious that both looseness and rub are changing with time (different data sets), which indicates the propagation of faults with time.

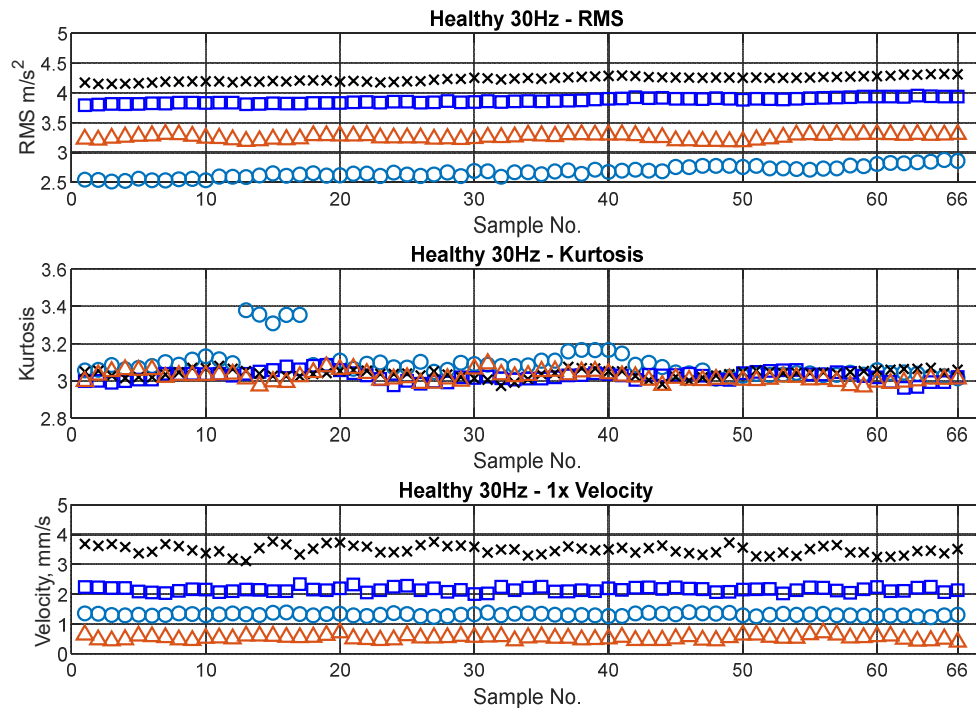


Figure 5. Estimated RMS and Kurtosis from the measured acceleration signals and their 1x velocity spectra values for the healthy condition at 1800 RPM (B1, circle; B2, square; B3, cross; and B4, triangle).

It is obvious from Figures 6–9 that there are significant changes in the vibration amplitudes due to the faults. There are some changes in the vibration values at 1x to 3x for each fault condition for different machine runs. These behaviours indicate that the faults may be propagating with the machine operation time. The change in vibration behaviour is found to be significant for both looseness and rub cases.

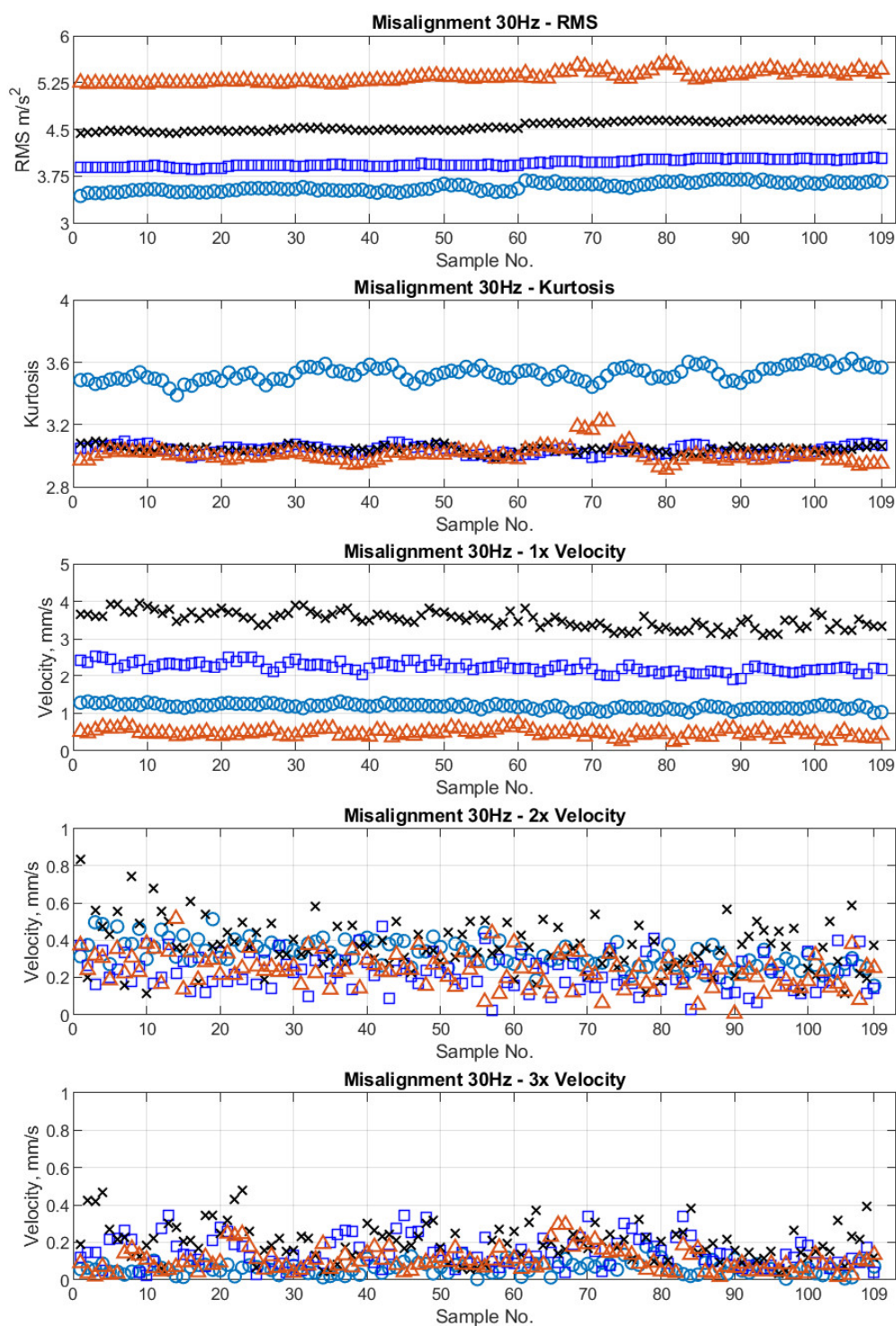


Figure 6. Estimated RMS and Kurtosis from the measured acceleration signals and their 1x, 2x, 3x velocity spectra values for the misalignment condition at 1800 RPM (B1, circle; B2, square; B3, cross; and B4, triangle).

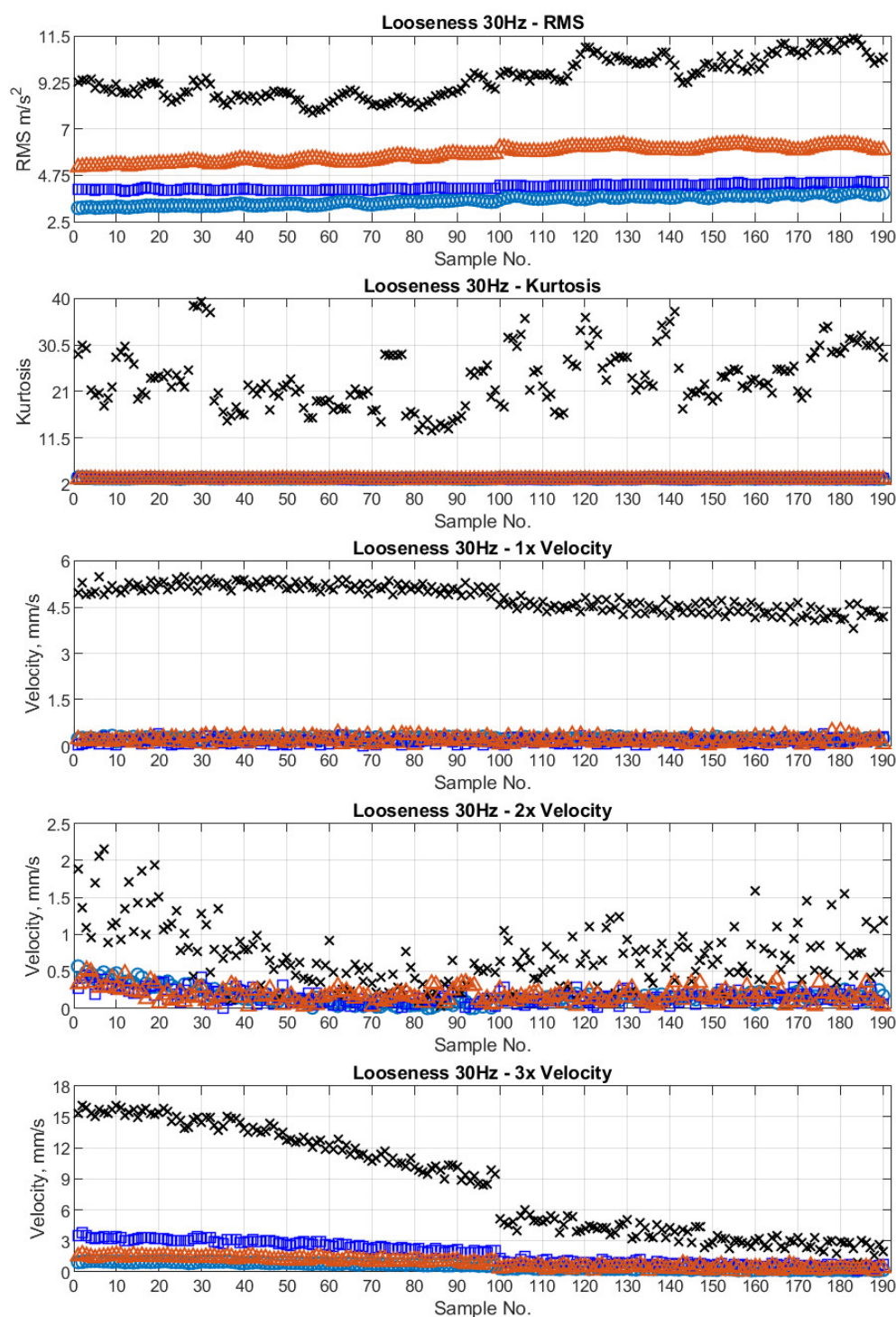


Figure 7. Estimated RMS and Kurtosis from the measured acceleration signals and their 1x, 2x, 3x velocity spectra values for the looseness condition at 1800 RPM (B1, circle; B2, square; B3, cross; and B4, triangle).

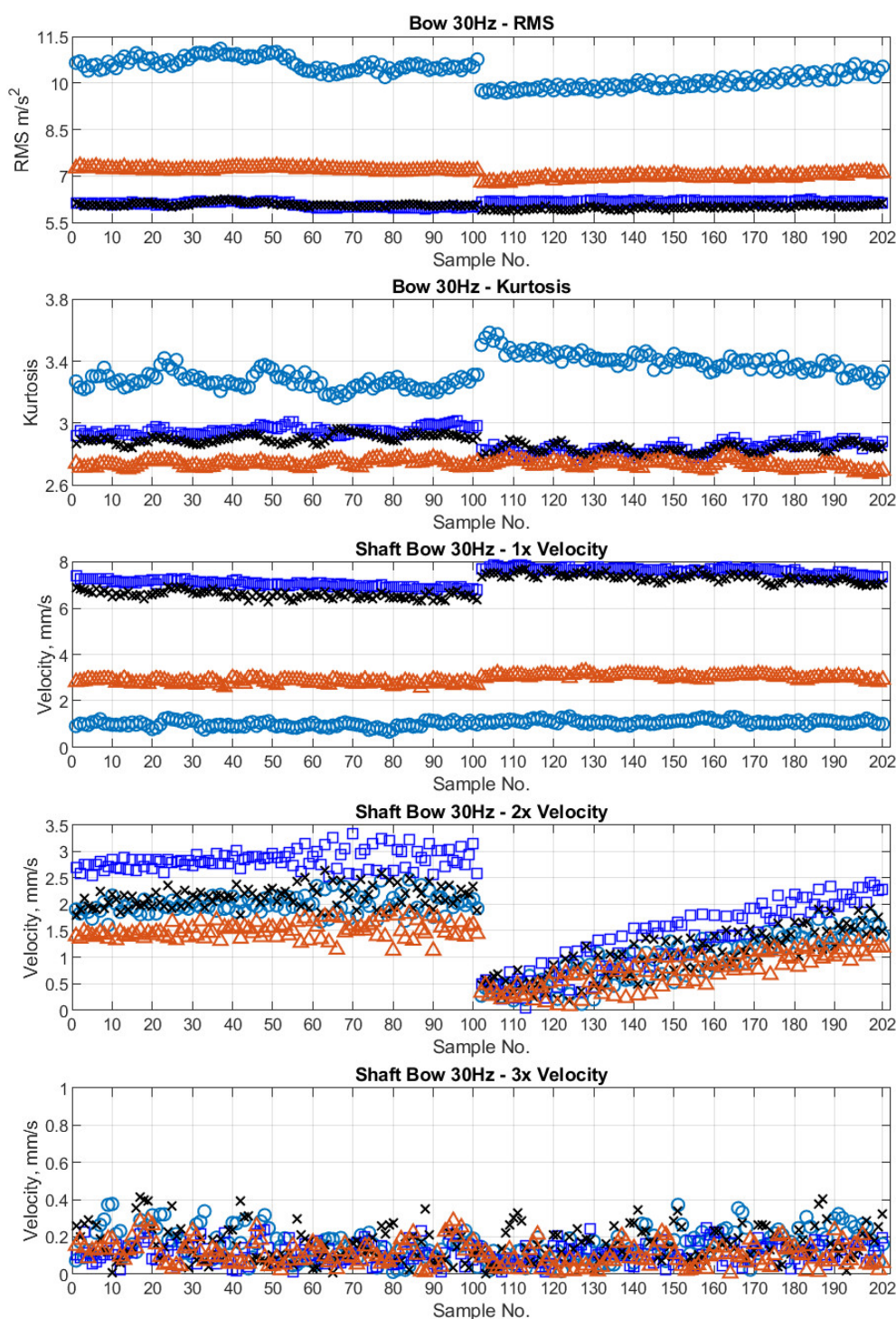


Figure 8. Estimated RMS and Kurtosis from the measured acceleration signals and their 1x, 2x, 3x velocity spectra values for the shaft bow condition at 1800 RPM (B1, circle; B2, square; B3, cross; and B4, triangle).

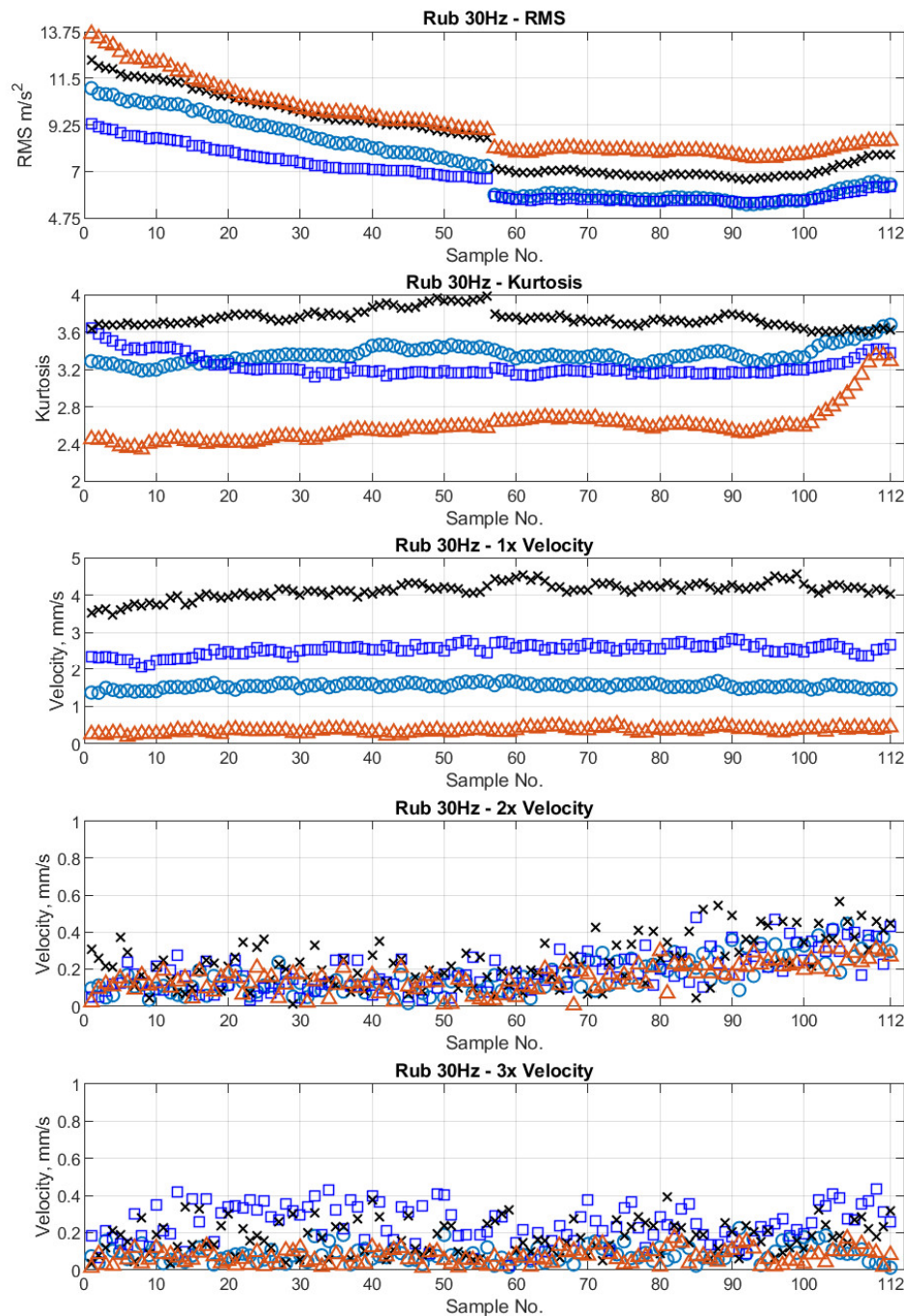


Figure 9. Estimated RMS and Kurtosis from the measured acceleration signals and their 1x, 2x, 3x velocity spectra values for the shaft rub condition at 1800 RPM (B1, circle; B2, square; B3, cross; and B4, triangle).

4.2. Rotor Speed: 2400 RPM (40 Hz)

Figures 10–14 show similar trend plots for the machine’s healthy and faulty conditions when operating at 2400 RPM. The observations are also similar to the behaviours observed at the machine speed of 1800 RPM.

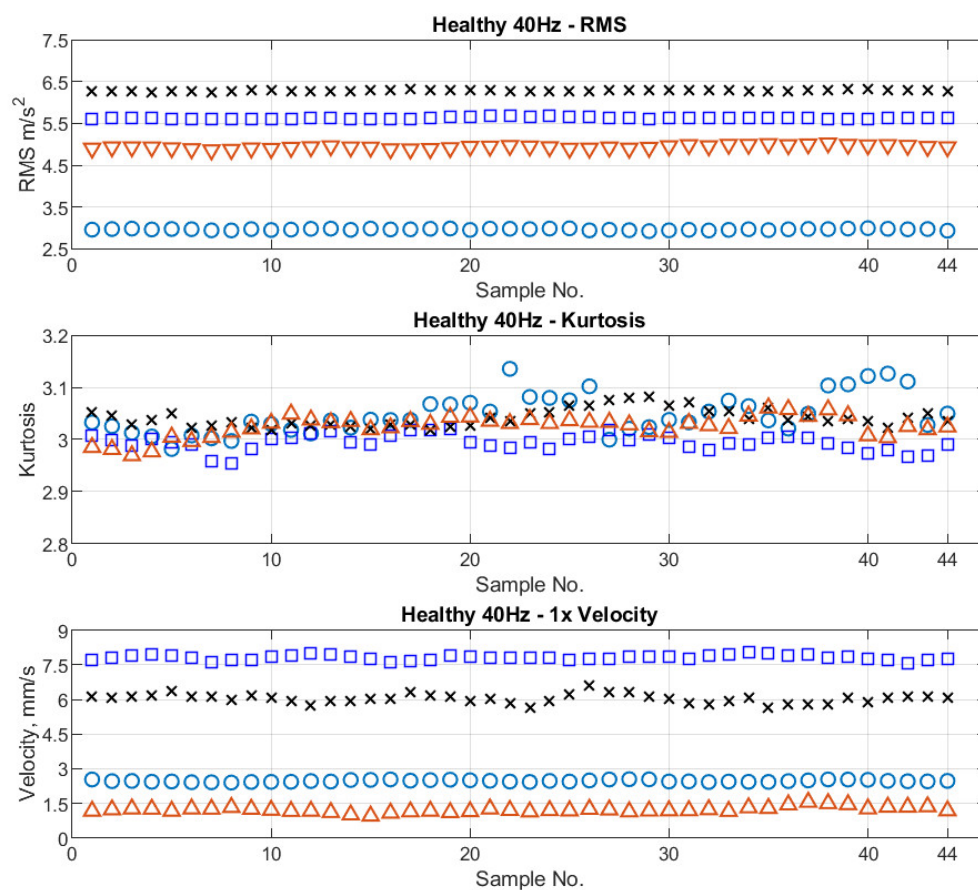


Figure 10. Estimated RMS and Kurtosis from the measured acceleration signals and their 1x velocity spectra values for the healthy condition at 2400 RPM (B1, circle; B2, square; B3, cross; and B4, triangle).

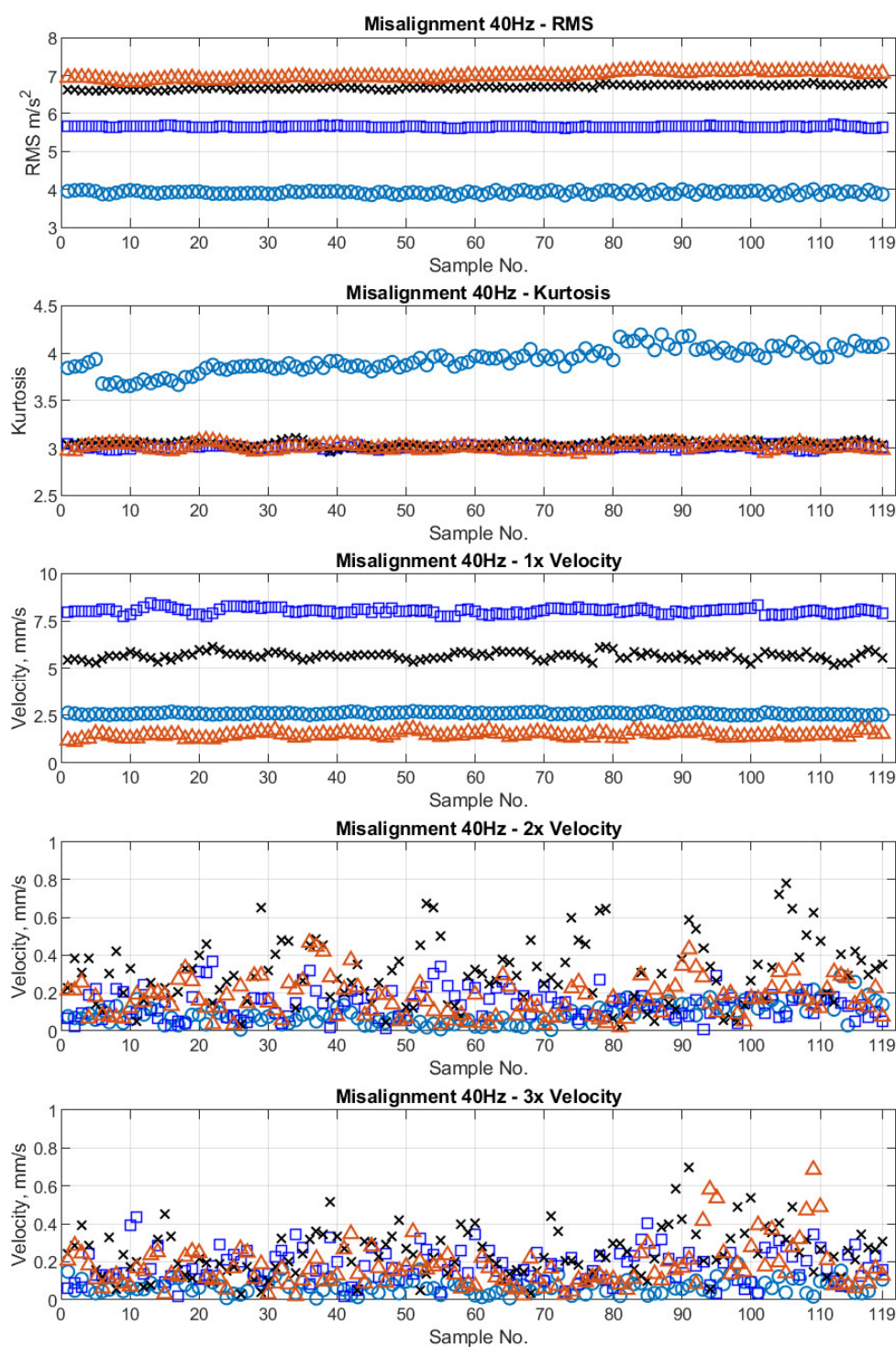


Figure 11. Estimated RMS and Kurtosis from the measured acceleration signals and their 1x, 2x, 3x velocity spectra values for the misalignment condition at 2400 RPM (B1, circle; B2, square; B3, cross; and B4, triangle).

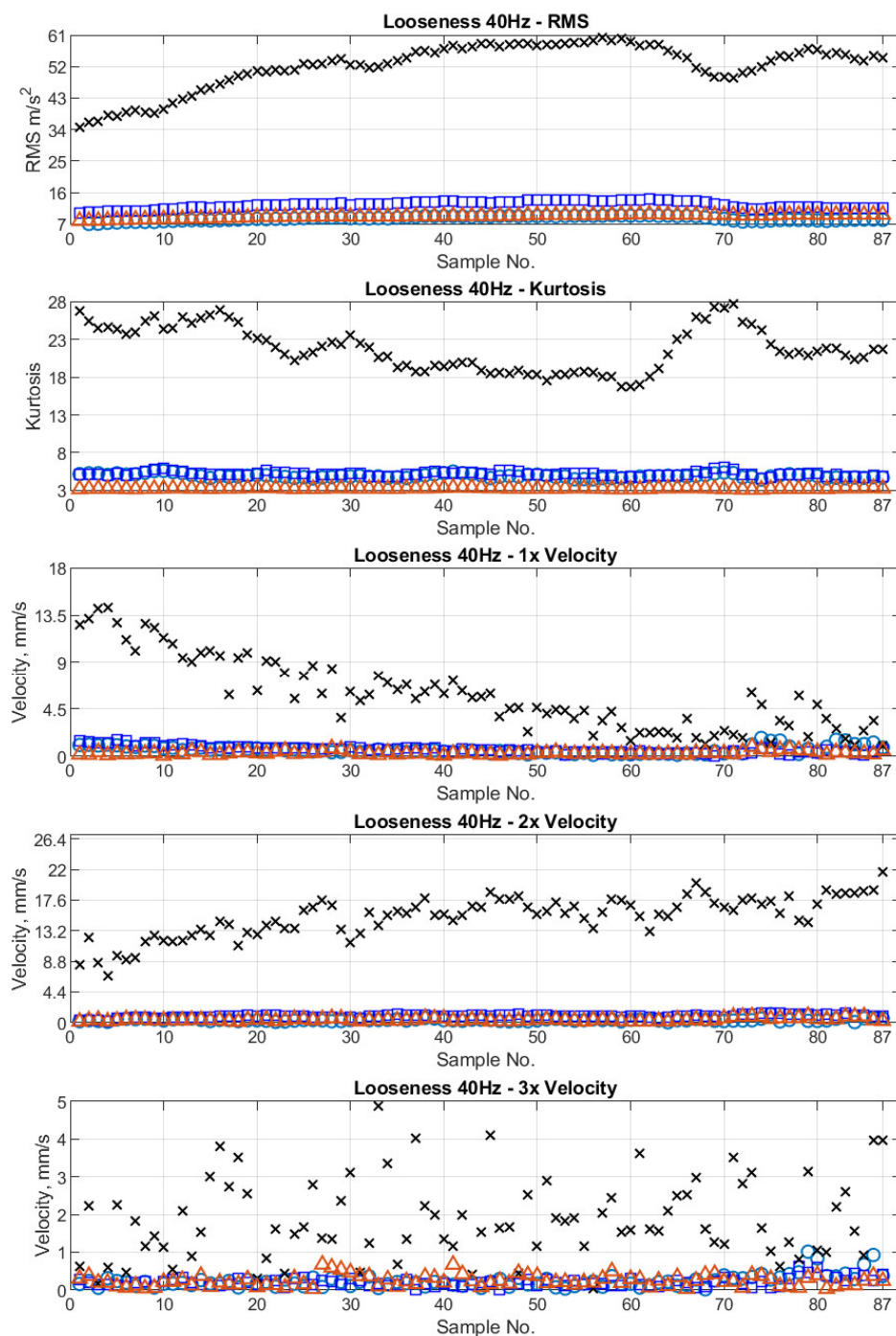


Figure 12. Estimated RMS and Kurtosis from the measured acceleration signals and their 1x, 2x, 3x velocity spectra values for the looseness condition at 2400 RPM (B1, circle; B2, square; B3, cross; and B4, triangle).

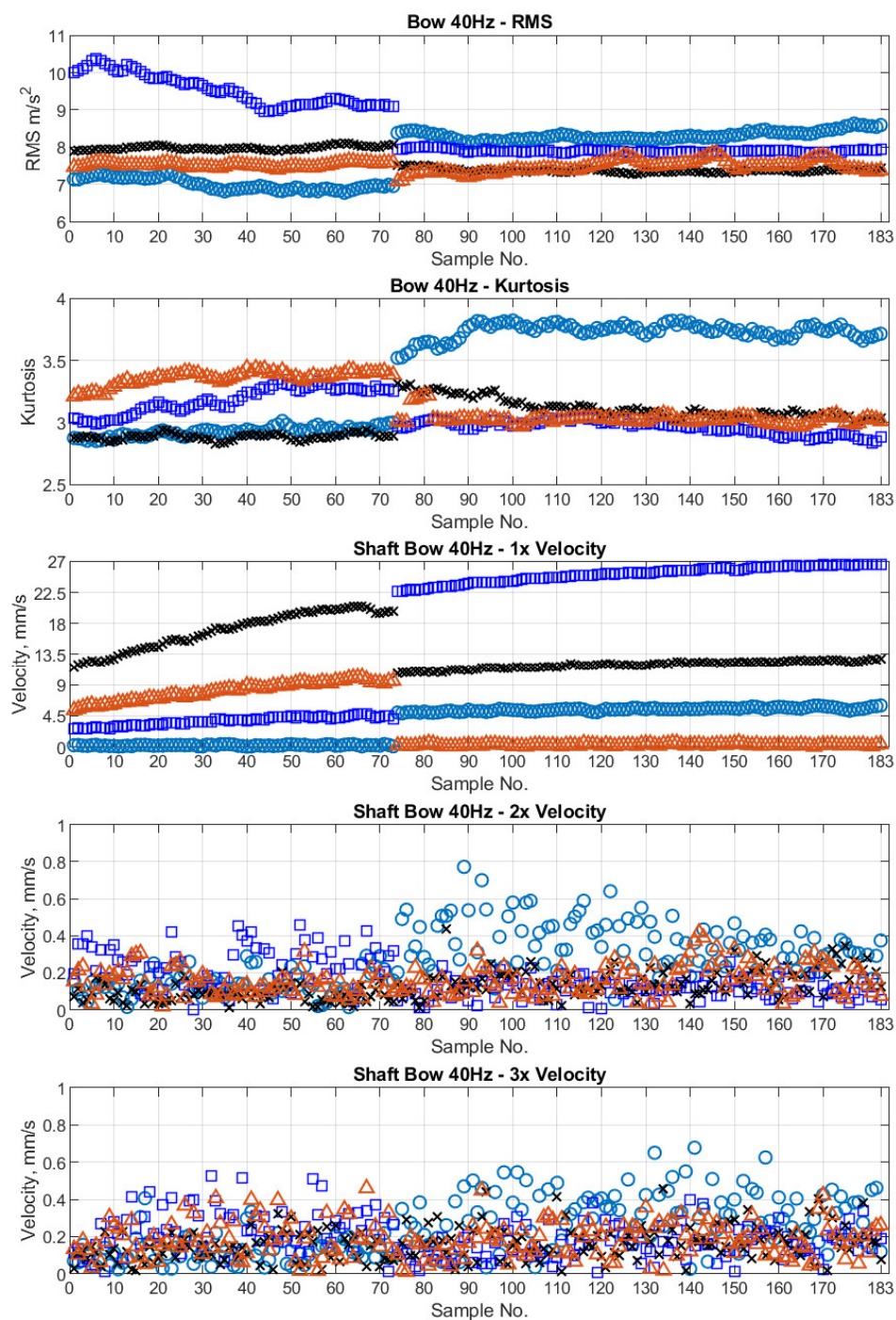


Figure 13. Estimated RMS and Kurtosis from the measured acceleration signals and their 1x, 2x, 3x velocity spectra values for the shaft bow condition at 2400 RPM (B1, circle; B2, square; B3, cross; and B4, triangle).

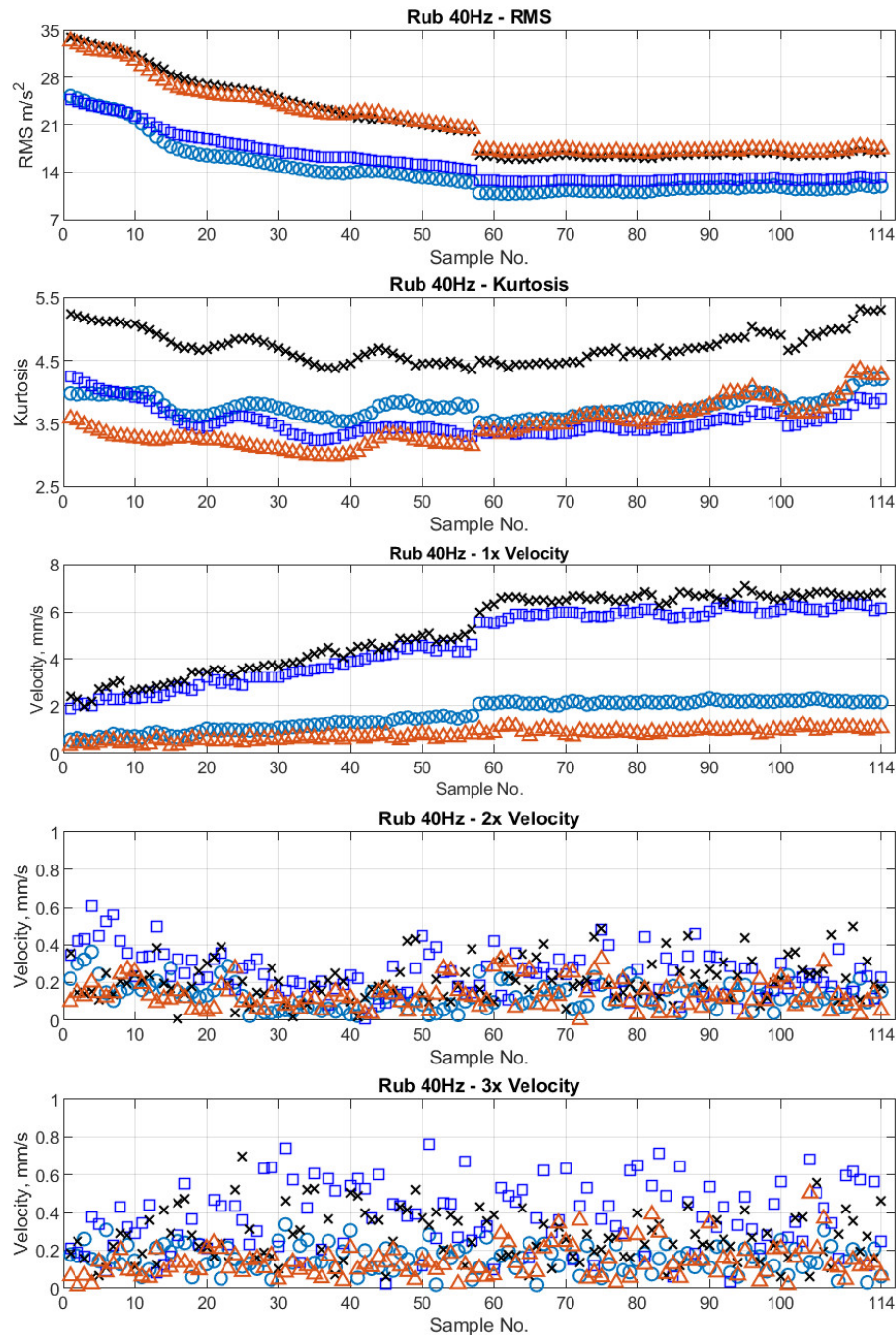


Figure 14. Estimated RMS and Kurtosis from the measured acceleration signals and their 1x, 2x, 3x velocity spectra values for the shaft rub condition at 2400 RPM (B1, circle; B2, square; B3, cross; and B4, triangle).

5. Parameter Optimisation

Since ANNs are not programmed, their performance depends on the quality and pre-processing of the input data, the network architecture and its design. Therefore, the meaningful input data representing the physics of the machine rotor dynamics are important for the successful development of the VML model.

In this study, the ANN approach discussed in Section 2 is used for the rotor dynamics physics-based input data estimated from the measured vibration data for the development of the VML model. The developed model can then be blindly applied and predict the machine fault accurately even when applied to other identical machines or a machine with different operation conditions or both, without

making any adjustments in the existing VML model, such as additional training and/or changing input parameters. This section presents a couple of the earlier models and their capabilities and accuracy when applied blindly to different machine operating conditions. Then, the paper proposes a model with the rotor dynamics physics-based optimised input parameters to enhance the blind fault diagnosis capabilities.

5.1. Approach 1: Time Domain Features

This is a recent study by the authors [25]. In this paper, only time domain features (or parameters) obtained from the measured vibration signals are used as the inputs to the VML model. The features used are the root mean square (RMS, represents the overall vibration amplitude), the variance (V , represents the signal power and non-zero mean of the vibration signals due to the presence of faults), the skewness (S , represents asymmetry signal nature), and the kurtosis (K , provides information about the shape distribution of the signals). These features provide useful information both qualitatively and quantitatively for any time domain data. Data inputs for i th run of the rig are prepared as

$$input_i = [RMS1_i \quad RMS2_i \quad RMS3_i \quad RMS4_i \quad V1_i \quad V2_i \quad V3_i \quad V4_i \quad S1_i \quad S2_i \quad S3_i \quad S4_i \quad K1_i \quad K2_i \quad K3_i \quad K4_i]^T,$$

where 1 to 4 represent the bearings B1 to B4, respectively. The VML model is developed as discussed in Section 4 with 100% accuracy in all sections—training, validation and testing for the input data at the machine speed of 1800 RPM (30 Hz). This model is then applied blindly for all runs (data sets) for the machine rotating speed of 2400 RPM (40 Hz), as listed in Table 2, without any training or tuning of the developed VML model at 1800 RPM. The performance results are listed in Table 3. The results are observed to be very good and show the potential to use this model for industrial cases. The VML model predicted the healthy, bow, looseness and rub conditions accurately. However, it fails to predict the misalignment accurately. This fault is diagnosed as the bow and looseness. This is still a positive sign for the model because this fault is not diagnosed as the healthy. This simply indicates the time domain features may not be sufficient to provide the rotor dynamics physics of each machine conditions.

Table 3. Blind application performance (%) at 2400 RPM of approach 1: time domain feature-based ML model.

Actual Diagnosis	Healthy	Misalignment	Bow	Looseness	Rub
Healthy	100.0	0.0	0.0	0.0	0.0
Misalignment	0.0	0.0	0.0	0.0	0.0
Bow	0.0	67.1	100.0	0.0	0.0
Looseness	0.0	0.0	0.0	100.0	0.0
Rub	0.0	32.9	0.0	0.0	100.0

5.2. Approach 2: Time–Frequency Domain Features

Nembhard, Sinha et al. [4] have used both time and frequency domain features for the development of a fault diagnosis model. The model has used the time domain features (RMS, crest factor (CF), Kurtosis (K)) and the frequency domain features (1x, 2x, ..., 5x amplitudes) of the acceleration signals. The study has successfully demonstrated the combinations of different machine speeds and the different machine foundations in the diagnostics model. However, the authors used all data simultaneously for the development of their model. Therefore, the model is not tested blindly. This model was then further modified by Luwei, Sinha et al. [26]. The features are slightly modified based on rotor dynamics. Since the velocity spectrum is better for the rotor-related faults [1], the frequency domain features are changed to the 1x, 2x, ..., 5x amplitudes of the velocity spectra [26]. It is observed that the classification and diagnosis of the different machine conditions are improved

further. These features are used again to develop the VML model as discussed in Section 2. Data inputs are prepared as

$$input_i = [RMS1_i \text{ CF1}_i \text{ K1}_i \text{ 1x1}_i \text{ 2x1}_i \text{ 3x1}_i \text{ 4x1}_i \text{ 5x1}_i \text{ RMS2}_i \dots \text{ 5x2}_i \text{ RMS3}_i \dots \text{ 5x3}_i \text{ RMS4}_i \dots \text{ 5x4}_i]^T.$$

Once again, the developed VML model is found to be 100% accurate during training, validation and testing for the input data at the machine speed of 1800 RPM (30 Hz). However, for the VML model when applied blindly to all runs (data sets) for the machine rotating speed at 2400 RPM (40 Hz), the diagnoses results are not good enough. The blind performance results are listed in Table 4. The performance of this model is significantly poorer than the time domain feature-based VML model.

Table 4. Blind application performance (%) at 2400 RPM of approach 2: time–frequency feature-based ML model.

Actual Diagnosis	Healthy	Misalignment	Bow	Looseness	Rub
Healthy	15.9	0.0	0.0	0.0	0.0
Misalignment	0.0	5.9	0.0	0.0	0.0
Bow	0.0	0.0	10.8	0.0	0.0
Looseness	0.0	0.0	0.0	1.1	0.0
Rub	84.1	94.1	89.2	98.9	100.0

5.3. Current Proposal

Further investigations are conducted on each feature to understand the success of approach 1 (time domain features) and the failure of approach 2 (both time and frequency domain features) VML models. It has been observed that the features of 4x and 5x amplitudes are not clearly seen in most cases and generally equivalent to the background noises. It is also observed that the feature crest factor (CF) is also changing significantly within the data set for the same machine condition. This is because the CF is heavily dependent on a single peak value of the acceleration signal. This may be one of the possible reason for the poorer performance of approach 2.

It is obvious from the observations that the time domain features (acceleration RMS and Kurtosis) and the frequency domain features (1x, 2x and 3x amplitudes of the velocity spectra) are good indicators that represent the machine dynamics. However, the faults, such as looseness and rub, may not be fully represented by these features. Both faults generally show the subharmonics and their higher harmonics [1,2]. The subharmonic peaks in the spectrum may not always appear at a fixed frequency; these may appear at 0.25x, 0.33x or 0.5x. Therefore, a spectrum energy (SE) between 5 Hz to 500 Hz from the velocity spectrum is also included in the feature list to represents the faults such as looseness and rub. Thus, the input features (acceleration (RMS and Kurtosis) and velocity (1x, 2x, 3x and SE)) are used in the proposed method. The inputs data for the development of the VML model are prepared as

$$input_i = [RMS1_i \text{ K1}_i \text{ 1x1}_i \text{ 2x1}_i \text{ 3x1}_i \text{ SE1}_i \text{ RMS2}_i \dots \text{ SE2}_i \text{ RMS3}_i \dots \text{ SE3}_i \text{ RMS4}_i \dots \text{ SE4}_i]^T$$

The VML model is again developed with 100% accuracy at the machine speed of 1800 RPM. This model is again blindly applied to all data sets listed in Table 2 at the machine speed of 2400 RPM. The performance results are listed in Table 5. The model predicted most of the machine conditions (both healthy and faulty) accurately in most cases, except in the case of the looseness fault, where just over 1% of cases were predicted as the rub fault. Therefore, this VML model with the rotor dynamics physics-based features seems robust for industrial application. Table 6 also provides a summary of the average central processing time (CPU) time for both training and diagnosis predictions (per input data) for the discussed three approaches. It is clear from Table 6 that the fault diagnosis can be performed quickly through the VML model.

Table 5. Blind application performance (%) at 2400 RPM of the proposed vibration-based machine learning (VML) model.

Actual Diagnosis \	Healthy	Misalignment	Bow	Looseness	Rub
Healthy	100.0	0.0	0.0	0.0	0.0
Misalignment	0.0	100.0	0.0	0.0	0.0
Bow	0.0	0.0	100.0	0.0	0.0
Looseness	0.0	0.0	0.0	98.9	0.0
Rub	0.0	0.0	0.0	1.1	100.0

Table 6. CPU time by different VML models.

Approaches	Total Training CPU Time (Seconds)	Blind Diagnosis CPU Time (Seconds/Sample)
Approach 1: only time domain features [25]	104.5156	0.1396
Approach 2: time domain and frequency domain features [26]	95.1250	0.1218
Proposed approach: optimised features	91.8125	0.1123

6. Concluding Remarks

AI-based ML models seem to be the future for many applications. A number of studies related to vibration-based faults diagnosis using ML approaches can also be found in the literature. However, most of studies are applied to one or two faults/defects only and are also not tested on either an identical another machine or in different machine operation conditions. However, such VML models must have capability that can be applied to any identical machines with different operating conditions to achieve future objectives of centralised monitoring using the Industrial Internet of Things (IIoT) concept. Therefore, rotor dynamics physics-based input features are important for the development of a reliable and robust VML model. This is demonstrated here through an experimental rig example with different machine conditions (healthy and faulty) and operating conditions. The selection of features based on the machine rotor dynamics significantly improves the developed VML model. The developed VML shows robustness in the prediction capabilities even when applied blindly to machine data from the different operating condition.

Author Contributions: N.E.S.: concept and all data analysis, J.S.: providing data, concept and supervision model. All authors have read and agreed to the published version of the manuscript.

Funding: This research received no external funding.

Acknowledgments: Jyoti K. Sinha acknowledges his PhD students and Keri Elbhah for the development of the rig, and Akilu Kaltungo and Adrian Nembhard for the experiments and experimental data that are used in this study. Natalia Fernanda Espinoza Sepúlveda acknowledges the support by CONICYT (Comisión Nacional de Investigación Científica y Tecnológica/Chilean National Commission for Scientific and Technological Research) “Becas Chile” Doctorate’s Fellowship programme; Grant No. 72190062 for her PhD study.

Conflicts of Interest: The authors declare no conflict of interest. The funders had no role in the design of the study; in the collection, analyses, or interpretation of data; in the writing of the manuscript, or in the decision to publish the results.

Abbreviations

AI	Artificial Intelligence
ANN	Artificial Neural Network
CNN	Convolution Neural Network
IIoT	Industrial Internet of Things

kNN	k-Nearest Neighbour
ML	Machine Learning
PCA	Principal Component Analysis
RMS	Root Mean Square
RPM	Rotation per Minute
SVM	Support Vector Machine
SVRM	Support Vector Regression Machine
TWSVM	Twin Support Vector Machine
VCN	Vibration-based Condition Monitoring
VFD	Vibration-based Fault Diagnosis
VML	Vibration-based Machine Learning

References

1. Sinha, J.K. *Industrial Approaches in Vibration-Based Condition Monitoring*, 1st ed.; Taylor & Francis, CRC Press, Boca Raton, FL, USA, 2020.
2. Sinha, J.K. *Vibration Analysis, Instruments, and Signal Processing*, 1st ed.; Taylor & Francis: CRC Press, Boca Raton, FL, USA, 2015.
3. Nembhard, A.D.; Sinha, J.K. Unified Multi-speed analysis (UMA) for the condition monitoring of aero-engines. *Mech. Syst. Signal Process.* **2015**, *64–65*, 84–99.
4. Nembhard, A.D.; Sinha, J.K.; Yunusa-Kaltungo, A. Development of a generic rotating machinery fault diagnosis approach insensitive to machine speed and support type. *J. Sound Vib.* **2015**, *337*, 321–341.
5. Belfiore, N.P.; Rudas, I.J. Applications of computational intelligence to mechanical engineering. In Proceedings of the IEEE 15th International Symposium on Computational Intelligence and Informatics (CINTI), Budapest, Hungary, 19–21 November 2014; pp. 351–368.
6. Liu, R.; Yang, B.; Zio, E.; Chen, X. Artificial intelligence for fault diagnosis of rotating machinery: A review. *Mech. Syst. Signal Process.* **2018**, *108*, 33–47.
7. Jiang, B.; Xiang, J.; Wang, Y. Rolling bearing fault diagnosis approach using probabilistic principal component analysis denoising and cyclic bispectrum. *J. Vib. Control* **2016**, *22*, 2420–2433.
8. Zhao, H.; Zheng, J.; Xu, J.; Deng, W. Fault diagnosis method based on principal component analysis and broad learning system. *IEEE Access* **2019**, *7*, 99263–99272.
9. De Moura, E.P.; Souto, C.R.; Silva, A.A.; Irmão, M.A.S. Evaluation of principal component analysis and neural network performance for bearing fault diagnosis from vibration signal processed by RS and DF analyses. *Mech. Syst. Signal Process.* **2011**, *25*, 1765–1772.
10. Shen, C.; Wang, D.; Liu, Y.; Kong, F.; Tse, P.W. Recognition of rolling bearing fault patterns and sizes based on two-layer support vector regression machines. *Smart Struct. Syst.* **2014**, *13*, 453–471.
11. Chen, Z.; Deng, S.; Chen, X.; Li, C.; Sanchez, R.V.; Qin, H. Deep neural networks-based rolling bearing fault diagnosis. *Microelectron. Reliab.* **2017**, *75*, 327–333.
12. Zhang, R.; Tao, H.; Wu, L.; Guan, Y. Transfer learning with neural networks for bearing fault diagnosis in changing working conditions. *IEEE Access* **2017**, *5*, 14347–14357.
13. Song, L.; Wang, H.; Chen, P. Vibration-based intelligent fault diagnosis for roller bearings in low-speed rotating machinery. *IEEE Trans. Instrum. Meas.* **2018**, *67*, 1887–1899.
14. Liu, Z.; Guo, W.; Hu, J.; Ma, W. A hybrid intelligent multi-fault detection method for rotating machinery based on RSGWPT, KPCA and twin SVM. *ISA Trans.* **2017**, *66*, 249–261.
15. Jia, F.; Lei, Y.; Guo, L.; Lin, J.; Xing, S. A neural network constructed by deep learning technique and its application to intelligent fault diagnosis of machines. *Neurocomputing* **2018**, *272*, 619–628.
16. Xia, M.; Li, T.; Xu, L.; Liu, L.; De Silva, C.W. Fault diagnosis for rotating machinery using multiple sensors and convolutional neural networks. *IEEE/ASME Trans. Mechatron.* **2018**, *23*, 101–110.
17. Huang, W.; Huang, J.; Yang, L.; Cao, C.; Chen, H. Fault diagnosis of gearbox based on principal component analysis and sequential probability ratio test. In Proceedings of the 2nd International Conference on Computer Science and Application Engineering, Hohhot, China, 22–24 October 2018; Volume 166, pp. 1–7.
18. Xing, Z.; Qu, J.; Chai, Y.; Tang, Q.; Zhou, Y. Gear fault diagnosis under variable conditions with intrinsic time-scale decomposition-singular value decomposition and support vector machine. *J. Mech. Sci. Technol.* **2017**, *31*, 545–553.

19. Yinghua, Y.; Guoqiang, S.; Xiang, S. Fault monitoring and classification of rotating machine based on PCA and KNN. In Proceedings of the 30th Chinese Control and Decision Conference, Shenyang, China, 9–11 June 2018; pp. 1795–1800.
20. Rapur, J.S.; Tiwari, R. Experimental time-domain vibration- based fault diagnosis of centrifugal pumps using support vector machine. *ASCE-ASME J. Risk Uncertain. Eng. Syst. Part B Mech. Eng.* **2017**, *3*, doi:10.1115/1.4035440.
21. Bordoloi, D.J.; Tiwari, R. Identification of suction flow blockages and casing cavitations in centrifugal pumps by optimal support vector machine techniques. *J. Braz. Soc. Mech. Sci. Eng.* **2017**, *39*, 2957–2968.
22. Walker, R.B.; Vayanat, R.; Perinpanayagam, S.; Jennions, I.K. Unbalance localization through machine nonlinearities using an artificial neural network approach. *Mech. Mach. Theory* **2014**, *75*, 54–66.
23. Mohammed, A.A.; Neilson, R.D.; Deans, W.F.; MacConnell, P. Crack detection in a rotating shaft using artificial neural networks and PSD characterization. *Meccanica* **2014**, *49*, 255–266.
24. Nahvi, H.; Esfahanian, M. Fault identification in rotating machinery using artificial neural networks. *Proc. Inst. Mech. Eng. Part C J. Mech. Eng. Sci. Febr.* **2005**, *219*, 141–158.
25. Espinoza Sepulveda, N.; Sinha, J.K. Blind Application of developed Smart Vibration-based Machine Learning (SVML) model for machine faults diagnosis to different machine conditions. *J. Vib. Eng. Technol.* **2020**, <https://doi.org/10.1007/s42417-020-00250-1>
26. Luwei, K.C.; Sinha, J.K.; Yunusa-kaltungo, A.; Elbhah, K. Data fusion of acceleration and velocity features (dFAVF) approach for fault diagnosis in rotating machines. In Proceedings of the 14th International Conference on Vibration Engineering and Technology of Machinery, Lisbon, Portugal, 10–13 September 2018; Volume 211, p. 21005.
27. Vyas, N. Artificial neural network design for fault identification in a rotor-bearing system. *Mech. Mach. Theory* **2001**, *36*, 157–175.
28. Tarassenko, L. *A Guide to Neural Computing Applications*; Elsevier: Amsterdam, The Netherlands, 1998.
29. Vogl, T.P.; Mangis, J.K.; Rigler, A.K.; Zink, W.T.; Alkon, D.L. Accelerating the convergence of the backpropagation method. *Biol. Cybern.* **1988**, *59*, 257–263.
30. Bishop, C.M. *Pattern Recognition and Machine Learning*; Springer: New York, NY, USA, 2006.

Publisher’s Note: MDPI stays neutral with regard to jurisdictional claims in published maps and institutional affiliations.



© 2020 by the authors. Licensee MDPI, Basel, Switzerland. This article is an open access article distributed under the terms and conditions of the Creative Commons Attribution (CC BY) license (<http://creativecommons.org/licenses/by/4.0/>).